Hindawi Publishing Corporation
Journal of Spectroscopy
Volume 2015, Article ID 563763, 8 pages
http://dx.doi.org/10.1155/2015/563763

Research Article

Pencil Beam Spectral Measurements of Ce, Ho, Yb, and Ba Powders for Potential Use in Medical Applications

N. Martini,[1] V. Koukou,[1] C. Michail,[2] P. Sotiropoulou,[1] N. Kalyvas,[2] I. Kandarakis,[2] G. Nikiforidis,[1] and G. Fountos[2]

[1]*Department of Medical Physics, Medical School, University of Patras, Rion, 265 00 Patras, Greece*
[2]*Radiation Physics, Materials Technology and Biomedical Imaging Laboratory, Department of Biomedical Engineering, Technological Educational Institute of Athens, Egaleo, 122 10 Athens, Greece*

Correspondence should be addressed to I. Kandarakis; kandarakis@teiath.gr

Received 29 October 2014; Revised 19 December 2014; Accepted 19 December 2014

Academic Editor: Eugen Culea

The aim of the present study was to obtain modified X-ray spectra, by using appropriate filter materials for use in applications such as dual energy X-ray imaging. K-edge filtering technique was implemented in order to obtain narrow energy bands for both dual- and single-kVp techniques. Three lanthanide filters (cerium, holmium, and ytterbium) and a filter outside lanthanides (barium), with low K-edge, were used to modify the X-ray spectra. The X-ray energies that were used in this work ranged from 60 to 100 kVp. Relative root mean square error (RMSE) and the coefficient of variation were used for filter selection. The increasing filter thicknesses led to narrower energy bands. For the dual-kVp technique, 0.7916 g/cm^2 Ho, 0.9422 g/cm^2 Yb, and 1.0095 g/cm^2 Yb were selected for 70, 80, and 90 kVp, respectively. For the single-kVp technique 0.5991 g/cm^2 Ce, 0.8750 g/cm^2 Ba, and 0.8654 g/cm^2 Ce were selected for 80, 90, and 100 kVp, respectively. The filtered X-ray spectra of this work, after appropriate modification, could be used in various X-ray applications, such as dual-energy mammography, bone absorptiometry, and digital tomosynthesis.

1. Introduction

The photon spectrum from a conventional X-ray tube consists of a broadband of energies [1]. In dual energy medical applications, a low- and a high-energy band are required [2–6]. In order to resolve the broadband spectrum into low- and high-energy bands, the following three methods can be used: (i) K-edge filtering [7, 8], (ii) kVp switching [9, 10], and (iii) the combination of both [8, 11].

In single-kVp techniques, only a single exposure is required with K-edge filtering for both energies to be present simultaneously in the radiation beam. Selective attenuation of photons, just above the absorption edge, creates a transmitted spectrum consisting of two relatively narrow energy bands after heavy filtration [12]. Single-kVp techniques are used in quantitative measurements such as bone densitometry.

Dual-kVp techniques employ two sequential measurements at different kilovoltages, typically with different filters between exposures. In this technique, K-edge filtering is used to remove selectively energy photons, above the K-edge, from the spectra, while lower-energy photons are also diminished due to their low penetrability. When K-edge filters are applied, narrower spectra are obtained compared with the spectra filtered with conventional filters. The use of K-edge lanthanide filtering in dual-kVp technique for the narrowing of the low-energy peak was suggested initially by Rutt [8]. The narrowing of the low kV-spectrum results in greater separability between the two peaks in spectra as well as decrease of beam hardening effects. Gustafsson et al. [11] suggested the use of K-edge lanthanide filter for both the low- and high-energy exposures to narrow both the low- and high-keV peaks in spectra. Simulation studies indicated that K-edge filtered spectra could be used to various X-ray applications, such as dual energy mammography, X-ray computed mammotomography (dual-kVp), and bone densitometry (single-kVp) [4–6, 13–15]. Several semiconductor detectors have been proposed for X-ray spectra measurements under clinical conditions [16–22].

Table 1: Areal density ranges of the used substances and the corresponding elements.

Substance	Substance areal density (g/cm^2)	Element areal density (g/cm^2)	Element density (g/cm^3)	Element thickness (μm)	Value layers
$BaCl_2(H_2O)_2$	0.6224–1.5561	0.3500–0.8750	3.500	1000–2500	162–793
CeO_2	0.0818–2.0443	0.0665–1.6643	6.657	100–2500	67–238
Ho_2O_3	0.5037–1.5112	0.4398–1.3193	8.795	500–1500	75–399
Yb_2O_3	0.3832–1.1495	0.3365–1.0095	6.730	500–1500	76–178

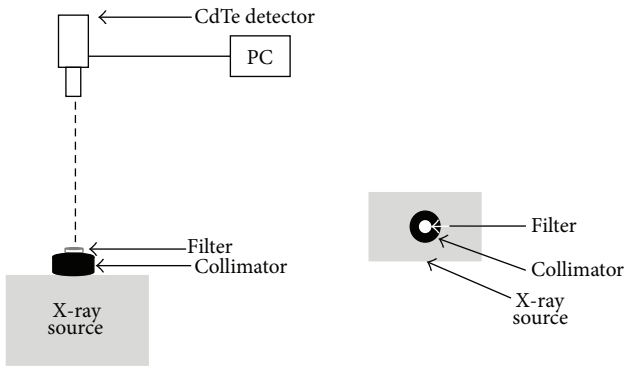

Figure 1: The set-up used for the spectra measurement.

In this paper, X-ray spectra filtered with several different powder filter materials were measured. A pencil beam was used, as the cone beam depends on the size and the position of the filter, as well as the broadening of the beam. In addition, when pencil beam is used, the divergence of the linear attenuation coefficient is minimized. A cadmium telluride (CdTe) energy discriminating and counting detector was used. K-edge filtering technique was implemented in order to obtain narrow energy bands, for both dual- and single-kVp techniques. The spectra presented here for the dual-kVp technique can be used in imaging techniques such as X-ray mammography, computed mammotomography, and angiography, while the spectra for the single-kVp technique can be used in bone densitometry for bone characterization.

2. Materials and Methods

X-ray spectroscopy was performed by measuring spectra from a tungsten (W) anode Norland XR-46 (Norland Medical Systems Inc., Fort Atkinson, WI). The tube voltage ranges from 60 to 100 kV. Five separate X-ray tube operating voltages, from 60 to 100 kVp, in 10 kV increments were investigated. The collimation applied was the standard collimation employed by Norland for dual energy X-ray absorptiometry (DEXA) applications. The divergence at a distance of 20.5 cm was 4 mm. The samarium (Sm) filter employed by Norland was extracted and replaced with the filters used in this study. Figure 1 shows the set-up used for the measurement of the spectra.

For the K-edge technique, barium (Ba), cerium (Ce), holmium (Ho), and ytterbium (Yb) were used, with their K-edge energies ranging from 37.44 to 61.33 keV. The Ce, Ho, and Yb filters were selected since they cover almost the whole atomic number (Z) range of lanthanides. The Ba filter material was, also, selected as an element outside lanthanides due to its lower K-edge. Elements with lower K-edge than Ba were not selected since they are eliminating the number of total counts in the low-energy peak in X-ray spectra. For the filtration with Ba, Ce, Ho, and Yb, barium chloride dihydrate ($BaCl_2(H_2O)_2$) (Mallinckrodt, 10326-17-9), cerium(IV) oxide (CeO_2) (Alfa Aesar, 44656, 99% purity), holmium(III) oxide (Ho_2O_3) (Sigma-Aldrich, H9750-10G, 99.9% purity), and ytterbium(III) oxide (Yb_2O_3) (Sigma-Aldrich, 246999-50G, 99% purity) powders were used, respectively. The areal densities of the substances ranged from 0.0818 to 2.0443 g/cm^2 corresponding to element (Ba, Ce, Ho, and Yb) thicknesses from 100 to 2500 μm, respectively (Table 1). The powders were prepared, by a mixture with pure carbon (7%) powder, in the form of 13 mm diameter discs (Figure 1), using an infrared spectroscopy hydraulic pellet press, by applying compression of 14 tons for 10 min. The mixture of the powders with the carbon was accomplished in order for the materials to be consistent. The acquisition parameters are summarized in Table 2. All the measurements had 5 min acquisition time. In the dual-kVp technique, Ce was used for the low energy and Ho and Yb were used for the high energy, while Ba and Ce filters were used for the single-kVp technique.

Table 2: Substances, kVp range, and exposure techniques used.

Substance	kVp	Technique
$BaCl_2(H_2O)_2$	80–100	Single-kVp
CeO_2	60–100	Dual- and single-kVp
Ho_2O_3	70–90	Dual-kVp
Yb_2O_3	70–90	Dual-kVp

The X-ray energy discriminating and counting detector system that was used for the spectroscopy measurements was a portable cadmium telluride (CdTe) detector (AMPTEK XR-100T) [23–26]. The CdTe detector was connected to a digital processor (PX4 Digital Pulse Processor), including three major components: (i) a high performance shaping amplifier, (ii) a multichannel analyzer (MCA), and (iii) power supplies. The detector was calibrated for energy scales, linearity checks, and energy resolution, by using ^{125}I (35 keV) and ^{99m}TC γ-ray (140.6 keV) calibration sources. The source to detector distance (SDD) was 47.5 cm.

The measured spectra were corrected for both efficiency and dead time of the PX4 multichannel analyzer in order to determine the incident photons on the detector surface. The efficiency of the XR-100CdTe results from the product

of the probability of transmission through beryllium (Be) window and the probability of the photon interactions within the active area of the CdTe detector. The data provided by the manufacturer were used for the detector efficiency corrections [27].

For all corrected measured spectra, relative root mean square error ($RMSE_{rel}$) was calculated as an indicative parameter of spectral energy bandwidth. The $RMSE_{rel}$ was used as a metric of the narrowing of the spectrum, since it calculates the divergence between values and in this case each energy, of the spectrum, from the corresponding mean energy [28]. $RMSE_{rel}$ can be expressed as

$$\mathrm{RMSE}_{\mathrm{rel}} = \sqrt{\frac{\sum_{E_{\min}}^{E_{\max}} \Phi(E_i)\left(E_i - \overline{E}\right)^2}{\sum_{E_{\min}}^{E_{\max}} \Phi(E_i) E_i}}, \quad (1)$$

where $\Phi(E_i)$ are the photons at each energy, E_i is the energy (keV), and $\overline{E}$ is the mean energy of the spectrum (keV).

The filters and the thickness range were chosen in order to fulfill both of the following criteria: (a) the narrowing of the energy band of the spectrum quantitated by $RMSE_{rel}$ and (b) the total number of photons in spectrum to exceed 10^6. When the total number of photons exceeds 10^6, the coefficient of variation (CV(%)) in this measurement will be less than 0.1% since the photon detection considers Poisson distribution and CV(%) was calculated from the following equation:

$$\mathrm{CV}\,(\%) = \frac{\sqrt{\sum \Phi(E_i)}}{\sum \Phi(E_i)} \cdot 100, \quad (2)$$

where $\Phi(E_i)$ are the photons at each energy E_i.

3. Results and Discussion

The results are presented as functions of the areal density of the corresponding element. Figure 2 shows measured spectra for 60 kVp, Ce filtered X-ray beam with areal densities of 0.4659 and 0.9319 g/cm^2, respectively. The 0.4659 g/cm^2 Ce filtered spectrum is plotted with continuous line, whereas the corresponding 0.9319 g/cm^2 is plotted with dashed lines. As it can be seen from Figure 2, the spectrum shape is not changing significantly, when increasing areal density, while the number of photons decreased to about 40%. Thicker filters reduce the number of lower-energy photons, while the high-energy photons are eliminated by the K-edge absorption [4–6]. Consequently, the mean energy of the filtered beam is concentrated around the K-edge of the filter material [12, 13].

Table 3 shows the $RMSE_{rel}$ and the CV(%) for the Ho and Yb filters used in 70, 80, and 90 kVp. At 70 kVp, 0.7916 g/cm^2 Ho and 0.8076 g/cm^2 Yb resulted in CV(%) approximately 0.1%. The Ho filter was selected as it had lower $RMSE_{rel}$ compared with Yb (7.14%). At 80 kVp, 0.7916 g/cm^2 Ho and 0.9422 g/cm^2 Yb fulfilled the limitation of CV(%). The Yb filter was selected as it resulted in 14.41% lower $RMSE_{rel}$. Finally, at 90 kVp, 0.8795 g/cm^2 Ho and 1.0095 g/cm^2 Yb resulted in CV(%) approximately 0.1%. However, the Yb had 37.74% lower $RMSE_{rel}$ compared with the Ho. Figures 3, 4, and 5 show the corresponding Ho and Yb filtered spectra at 70, 80, and 90 kVp, respectively. In Figures 3, 4, and 5, a small number of counts at energies over the K-edge were measured which are not visible in these plots. However, at 90 kVp Ho filtered spectrum (Figure 5), a number of counts at energies over the K-edge are noticeable, since the K absorption edge of Ho is lower than that of Yb. In Table 4, the selected

Table 3: Filters used in dual-kVp technique.

kVp (keV)	Areal density (g/cm^2)		$RMSE_{rel}$		CV (%)	
	Ho	Yb	Ho	Yb	Ho	Yb
70	0.7619	0.8076	0.0112	0.0120	0.1018	0.0980
80	0.7619	0.9422	0.0118	0.0101	0.0931	0.1035
90	0.8795	1.0095	0.0159	0.0099	0.1067	0.1035

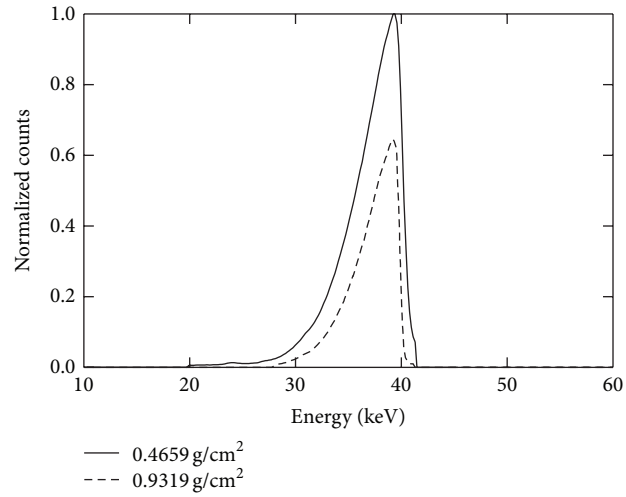

Figure 2: Low-energy spectrum at 60 kVp filtered with 0.4659 and 0.9319 g/cm^2 Ce (700 and 1400 μm Ce, resp.).

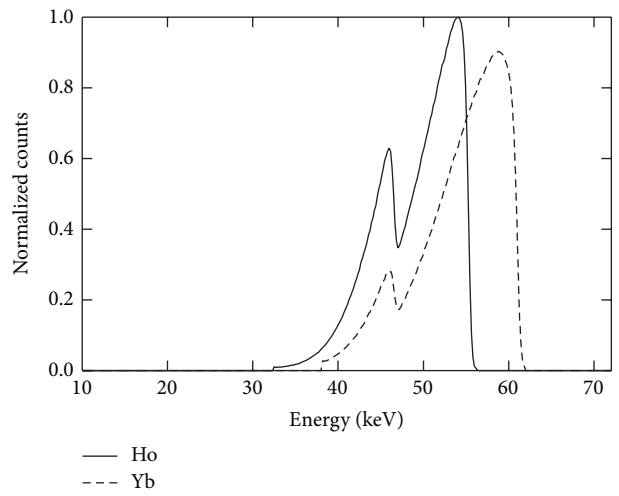

Figure 3: High-energy spectrum at 70 kVp filtered with 0.7916 g/cm^2 Ho and 0.8076 g/cm^2 Yb (900 μm Ho and 1200 μm Yb).

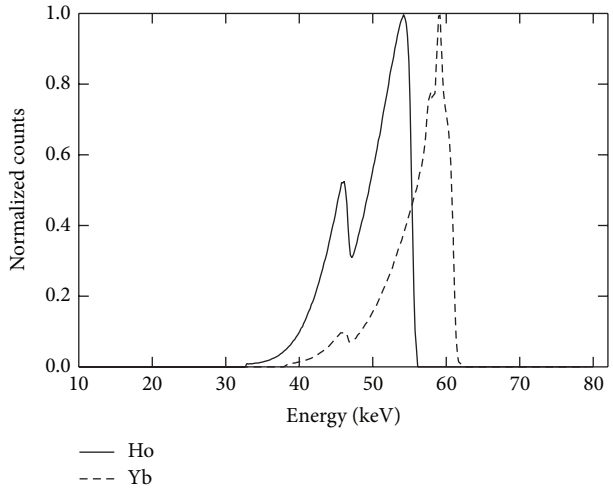

Figure 4: High-energy spectrum at 80 kVp filtered with 0.7916 g/cm^2 Ho and 0.9422 g/cm^2 Yb (900 μm Ho and 1400 μm Yb).

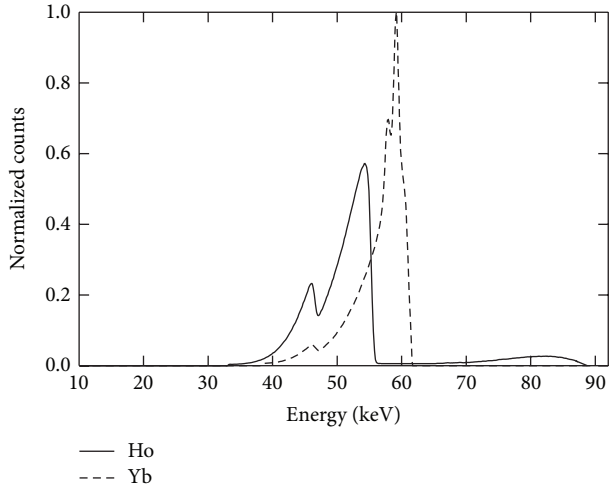

Figure 5: High-energy spectrum at 90 kVp filtered with 0.8795 g/cm^2 Ho and 1.0095 g/cm^2 Yb (1000 μm Ho and 1500 μm Yb).

filters for dual-kVp technique at 70, 80, and 90 kVp are shown. The mean energies, ME, were calculated as ME = $\sum \Phi(E_i)E_i / \sum \Phi(E_i)$, where $\Phi(E_i)$ are the photons at each energy E_i, for energies from 30 to 65 keV.

Figure 6 shows an 80 kVp X-ray spectrum filtered with 0.5991 g/cm^2 Ce for the single-kVp technique. A comparison of the filtered beams, at 60 kVp (Figure 2) and 80 kVp (Figure 6), shows that the high-energy photons result in a bimodal shape of the spectrum, by allowing higher-energy photon to pass through [12–14].

Figure 7 shows a 90 kVp spectrum filtered with 0.8750 g/cm^2 Ba. A sharp cutoff is evident in the detected photons at energies higher than the K-edge, leading to a spectrum with narrower energy bands. This spectrum, compared with a 0.8400 g/cm^2 Ba filtered spectrum, resulted in

Table 4: Mean and maximum energies for the selected dual-kVp filters.

kVp (keV)	Element	Areal density (g/cm^2)	Mean energy (keV)	Maximum energy (keV)
70	Ho	0.7619	50.31	55
80	Yb	0.9422	56.13	61
90	Yb	1.0095	56.89	61

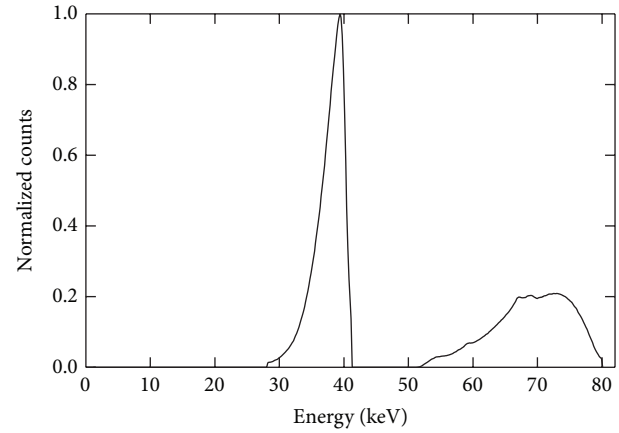

Figure 6: High-energy spectrum at 80 kVp filtered with 0.5991 g/cm^2 Ce (900 μm Ce).

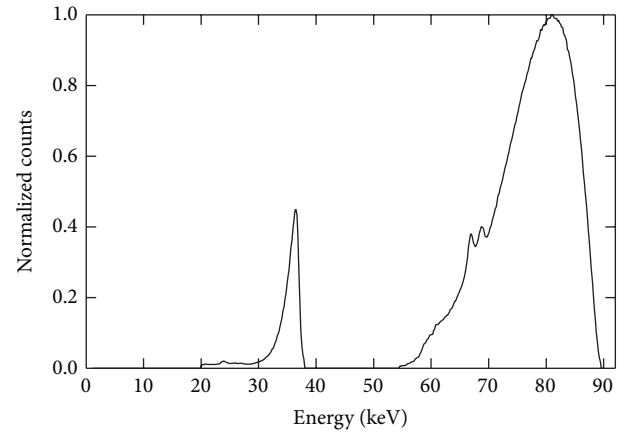

Figure 7: High-energy spectrum at 90 kVp filtered with 0.8750 g/cm^2 Ba (2500 μm Ba).

2.47% and 3.19% decreased $RMSE_{rel}$ in the low and the high peak, respectively.

Figure 8 shows 100 kVp spectra filtered with 0.8654 g/cm^2 Ce and 0.7700 g/cm^2 Ba. The low peak of Ba is narrower than the low peak of Ce, while the total number of counts in CeO_2 filtration was 9.46 times higher in the low peak.

Table 5 summarizes the ranges of mean energies of the substances used in each technique (dual- or single-kVp) and the kVps. In dual-kVp technique, the mean energies of the low- and high-energy band ranged from 35.05 to 37.65 keV and 48.16 to 56.89 keV, respectively, while for the single-kVp technique they ranged from 34.01 to 39.13 keV and 63.93 to

Table 5: Summarized mean energy values for both exposure techniques.

Technique	Substance	kVp	Thickness (μm)	Mean energy range (keV)	
				Low energy	High energy
Dual-kVp	CeO_2	60	100–1000	35.05–37.65	—
	Ho_2O_3	70	500–1500	—	48.16–51.92
		80		—	49.12–52.10
		90		—	50.91–52.46
	Yb_2O_3	70	500–1500	—	50.39–55.56
		80		—	52.15–56.38
		90		—	53.87–56.89
Single-kVp	CeO_2	80	1000–2500	37.72–39.12	68.39–73.27
		90		37.75–39.12	74.69–81.02
		100		37.75–39.13	80.74–88.36
	$BaCl_2(H_2O)_2$	80	1000–2500	34.01–35.49	63.93–69.54
		90		34.05–35.51	68.82–70.06
		100		34.08–35.52	73.43–82.34

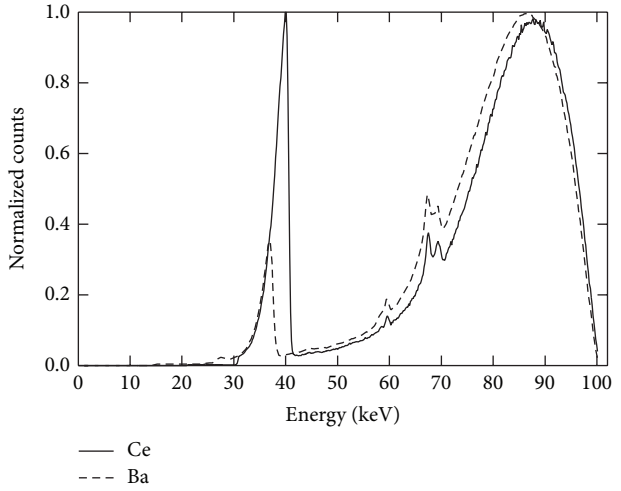

Figure 8: High-energy spectra at 100 kVp filtered with 0.8654 g/cm^2 Ce and 0.7700 g/cm^2 Ba (1300 μm Ce and 2200 μm Ba).

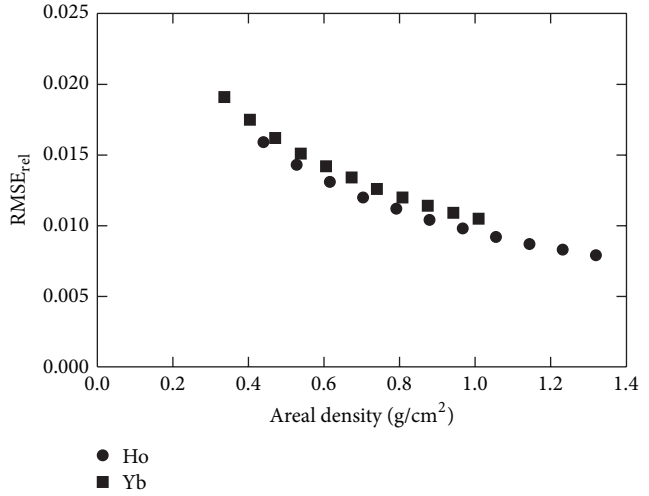

Figure 9: RMSE$_{rel}$ values as a function of areal density for all filters used in the dual-kVp technique at 70 kVp.

88.16 keV for the low- and high-energy band, respectively. This wide range, especially in high energy, indicates that these spectra could be used in several X-ray applications that are of interest in these energies, such as dual energy mammography and dual energy X-ray absorptiometry or even the mass calcium to phosphorus ratio determination in biological hydroxyapatite [4–6, 29].

RMSE$_{rel}$ values are plotted as a function of areal density for all filters used in the dual-kVp technique and are shown in Figures 9, 10, and 11 corresponding to 70, 80, and 90 kVp. It can be seen that, at 70 and 80 kVp, both filters had the same impact on the spectral width, over all areal density ranges. On the contrary, at 90 kVp, Yb minimizes the RMSE$_{rel}$ over all areal density ranges, since the K-edge absorption energy of Yb is higher than the K-edge of Ho filter.

Furthermore, for the single-kVp technique, the RMSE$_{rel}$ values are plotted as a function of areal density for all filters

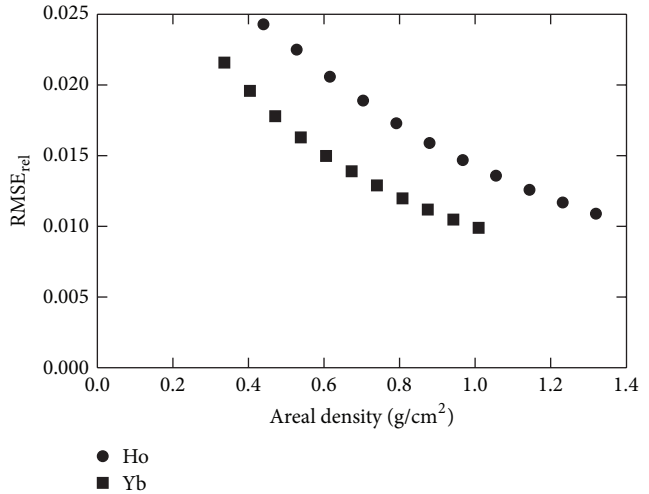

Figure 10: RMSE$_{rel}$ values as a function of areal density for all filters used in the dual-kVp technique at 80 kVp.

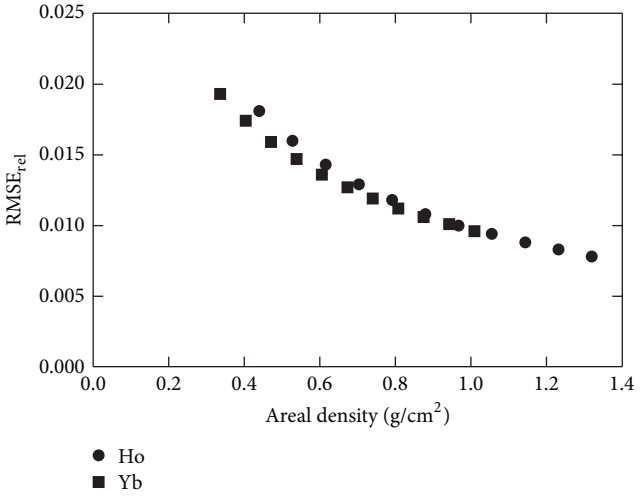

Figure 11: RMSE$_{rel}$ values as a function of areal density for all filters used in the dual-kVp technique at 90 kVp.

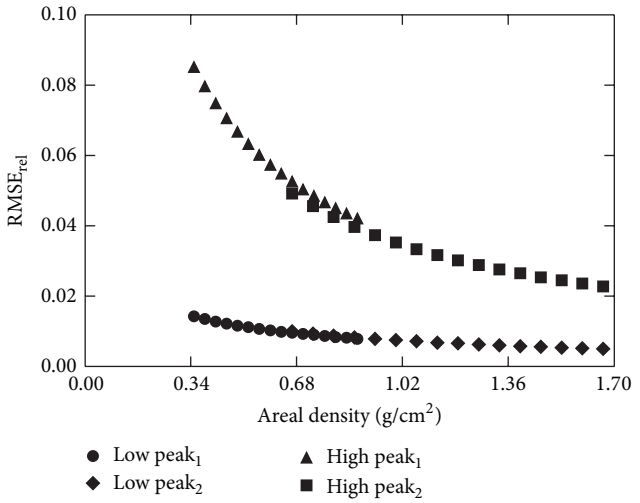

Figure 12: RMSE$_{rel}$ values as a function of areal density for all filters used in the single-kVp technique at 80 kVp (subscript 1 referred to Ba and 2 to Ce).

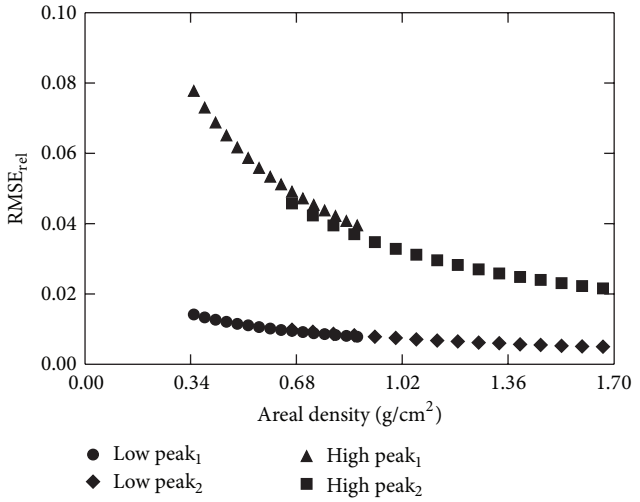

Figure 13: RMSE$_{rel}$ values as a function of areal density for all filters used in the single-kVp technique at 90 kVp (subscript 1 referred to Ba and 2 to Ce).

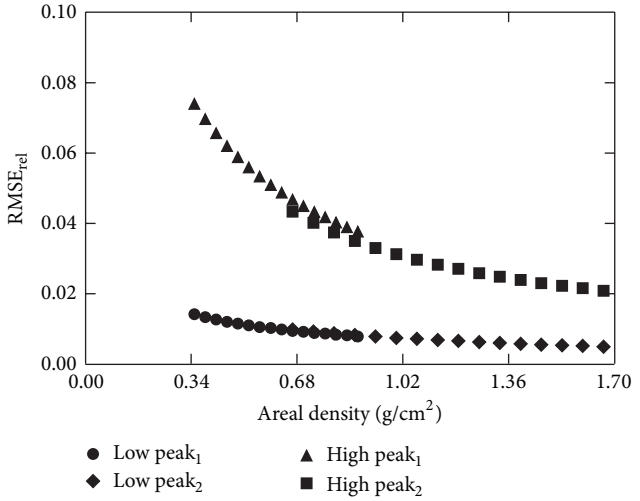

Figure 14: RMSE$_{rel}$ values as a function of areal density for all filters used in the single-kVp technique at 100 kVp (subscript 1 referred to Ba and 2 to Ce).

tested shown in Figures 12, 13, and 14, corresponding to 80, 90, and 100 kVp. As the areal density increases, lower RMSE$_{rel}$ values of the high-energy peak indicate that narrower beams can be obtained by using either Ce or Ba filter materials. Similar results were observed in previous studies [12, 14].

Using narrow energy X-ray beams, instead of wide energy X-rays, has several advantages in medical applications. Generally, in X-ray tubes inherent and added filtration is used to suppress the low-energy portion of the spectra. Low energies contribute to radiation dose, which increases the probability of cancer. Therefore, dose reduction at X-ray applications, that is, X-ray mammography, computed mammotomography, and computed tomography, would benefit the patients. Furthermore, using narrow beams, in dual energy techniques, is expected to improve separation of tissues with very small differences in attenuation coefficients or possibly the ability of noninvasive tissue characterization [3, 12–14, 29]. Also, imaging with narrow energy spectra provides lower scatter noise and as a result beneficial influence on image contrast and signal-to-noise ratio [2, 13, 14]. Heavy K-edge filtering used in this study indicated that elimination of low-energy photons was accomplished for both dual- and single-kVp techniques, leading to narrow energy bands. However, this technique reduces photon influence, (value layers in Table 1), and thus higher output X-ray tubes are required.

The spectra presented here for the dual-kVp technique can be used in imaging techniques, while the spectra for the single-kVp technique can be used in quantitative bone densitometry measurements and imaging using silicon strip photon counting detectors [30].

Mean energy range of the spectra was in the diagnostic X-ray energy range indicating that these spectra could be useful in various medical applications such as mammography, computed mammotomography, angiography, and DEXA.

4. Conclusions

In the present study, pencil X-ray beams were measured and filtered with different filter materials. K-edge filtering was implemented in order to obtain narrow energy bands for both dual- and single-kVp techniques. The increasing filter thickness resulted in narrowing of the spectral energy band, while on the contrary the total number of photons decreased. The X-ray tube voltages used in this work ranged from 60 to 100 kVp providing higher mean beam energies. The resulting mean energies, after filtration, indicate that these X-ray spectra could be used in various X-ray applications, such as dual energy mammography and absorptiometry and digital tomosynthesis improving their efficiency.

Conflict of Interests

The authors declare that there is no conflict of interests regarding the publication of this paper.

Acknowledgments

This research has been cofunded by the European Union (European Social Fund) and Greek national resources under the framework of the "Archimedes III: Funding of Research Groups in TEI of Athens" project of the "Education and Lifelong Learning" Operational Programme.

References

[1] R. Jonson, B. Roos, and T. Hansson, "Bone mineral measurement with a continuous roentgen ray spectrum and a germanium detector," *Acta Radiologica: Diagnosis*, vol. 27, no. 1, pp. 105–109, 1986.

[2] M. R. Lemacks, S. C. Kappadath, C. C. Shaw, X. Liu, and G. J. Whitman, "A dual-energy subtraction technique for microcalcification imaging in digital mammography—a signal-to-noise analysis," *Medical Physics*, vol. 29, no. 8, pp. 1739–1751, 2002.

[3] G. Fountos, S. Yasumura, and D. Glaros, "The skeletal calcium/phosphorus ratio: a new in vivo method of determination," *Medical Physics*, vol. 24, no. 8, pp. 1303–1310, 1997.

[4] V. Koukou, N. Martini, G. Fountos et al., "Calcification detection optimization in dual energy mammography: influence of the X-ray spectra," in *XIII Mediterranean Conference on Medical and Biological Engineering and Computing 2013: MEDICON 2013, 25–28 September 2013, Seville, Spain*, vol. 41 of *IFMBE Proceedings*, pp. 459–462, Springer International Publishing, Cham, Switzerland, 2014.

[5] P. Sotiropoulou, G. Fountos, N. Martini et al., "X-ray spectra for bone quality assessment using energy dispersive counting and imaging detectors with dual energy method," in *XIII Mediterranean Conference on Medical and Biological Engineering and Computing 2013*, vol. 41 of *IFMBE Proceedings*, pp. 463–466, Springer, 2014.

[6] V. Koukou, N. Martini, P. Sotiropoulou et al., "Modified polyenergetic X-ray spectra for dual energy method," *e-Journal of Science & Technology*, vol. 7, no. 3, pp. 79–85, 2012.

[7] B. Jacobson, "Development of dichromography techniques," Final Progress Report, Grant no. 5, The National Institute of Arthritis and Metabolic Diseases, 1968.

[8] B. K. Rutt, "Optimized KVP filtration and detection parameters for dual energy imaging," *Medical Physics*, vol. 2, no. 536, 1985.

[9] K. Reiss, K. Killig, and W. Schuster, "Dual photon x-ray beam applications," in *Proceedings of the International Conference on Bone Mineral Measurement*, R. Mazess, Ed., pp. 80–87, 1973.

[10] J. A. Sorenson, P. R. Duke, and S. W. Smith, "Simulation studies of dual-energy x-ray absorptiometry," *Medical Physics*, vol. 16, no. 1, pp. 75–80, 1989.

[11] L. Gustafsson, B. Jacobson, and L. Kusoffsky, "X-ray spectrophotometry for bone mineral determinations," *Medical and Biological Engineering*, vol. 12, no. 1, pp. 113–119, 1974.

[12] D. J. Crotty, R. L. McKinley, and M. P. Tornai, "Experimental spectral measurements of heavy *K*-edge filtered beams for x-ray computed mammotomography," *Physics in Medicine and Biology*, vol. 52, no. 3, pp. 603–616, 2007.

[13] R. L. McKinley, M. P. Tornai, E. Samei, and M. L. Bradshaw, "Simulation study of a quasi-monochromatic beam for x-ray computed mammotomography," *Medical Physics*, vol. 31, no. 4, pp. 800–813, 2004.

[14] S. J. Glick, S. Thacker, X. Gong, and B. Liu, "Evaluating the impact of x-ray spectral shape on image quality in flat-panel CT breast imaging," *Medical Physics*, vol. 34, no. 5, pp. 5–24, 2007.

[15] C. M. Michail, N. E. Kalyvas, I. G. Valais et al., "Figure of image quality and information capacity in digital mammography," *BioMed Research International*, vol. 2014, Article ID 634856, 11 pages, 2014.

[16] T. R. Fewell and R. E. Shuping, "Photon energy distribution of some typical diagnostic x-ray beams," *Medical Physics*, vol. 4, no. 3, pp. 187–197, 1977.

[17] R. Birch and M. Marshall, "Computation of bremsstrahlung X-ray spectra and comparison with spectra measured with a Ge(Li) detector," *Physics in Medicine and Biology*, vol. 24, no. 3, pp. 505–517, 1979.

[18] K. Aoki and M. Koyama, "Measurement of diagnostic x-ray spectra using a silicon photodiode," *Medical Physics*, vol. 16, no. 4, pp. 529–536, 1989.

[19] A. R. Chourasia, J. L. Hickman, R. L. Miller, G. A. Nixon, and M. A. Seabolt, "X-ray photoemission study of the oxidation of hafnium," *International Journal of Spectroscopy*, vol. 2009, Article ID 439065, 6 pages, 2009.

[20] S. Miyajima, K. Imagawa, and M. Matsumoto, "CdZnTe detector in diagnostic x-ray spectroscopy," *Medical Physics*, vol. 29, no. 7, pp. 1421–1429, 2002.

[21] S. Miyajima, "Thin CdTe detector in diagnostic x-ray spectroscopy," *Medical Physics*, vol. 30, no. 5, pp. 771–777, 2003.

[22] S. Stumbo, U. Bottigli, B. Golosio, P. Oliva, and S. Tangaro, "Direct analysis of molybdenum target generated x-ray spectra with a portable device," *Medical Physics*, vol. 31, no. 10, pp. 2763–2770, 2004.

[23] C. M. Michail, V. A. Spyropoulou, G. P. Fountos et al., "Experimental and theoretical evaluation of a high resolution CMOS based detector under X-ray imaging conditions," *IEEE Transactions on Nuclear Science*, vol. 58, no. 1, pp. 314–322, 2011.

[24] C. M. Michail, G. P. Fountos, I. G. Valais et al., "Evaluation of the red emitting Gd_2O_2S: Eu powder scintillator for use in indirect X-ray digital mammography detectors," *IEEE Transactions on Nuclear Science*, vol. 58, no. 5, pp. 2503–2511, 2011.

[25] I. E. Seferis, C. M. Michail, I. G. Valais et al., "On the response of a europium doped phosphor-coated CMOS digital imaging detector," *Nuclear Instruments and Methods in Physics Research Section A: Accelerators, Spectrometers, Detectors and Associated Equipment*, vol. 729, pp. 307–315, 2013.

[26] L. Abbene, A. La Manna, F. Fauci, G. Gerardi, S. Stumbo, and G. Raso, "X-ray spectroscopy and dosimetry with a portable CdTe device," *Nuclear Instruments and Methods in Physics Research Section A: Accelerators, Spectrometers, Detectors and Associated Equipment*, vol. 571, no. 1-2, pp. 373–377, 2007.

[27] Amptek, *X-Ray & Gamma Ray Detector*, XR-100T-CdTe [Internet], Amptek, Bedford, Mass, USA, 2014, http://www.amptek.com/xr100cdt.html.

[28] G. P. Fountos, C. M. Michail, A. Zanglis et al., "A novel easy-to-use phantom for the determination of MTF in SPECT scanners," *Medical Physics*, vol. 39, no. 3, pp. 1561–1570, 2012.

[29] G. Fountos, M. Tzaphlidou, E. Kounadi, and D. Glaros, "In vivo measurement of radius calcium/phosphorus ratio by x-ray absorptiometry," *Applied Radiation and Isotopes*, vol. 51, no. 3, pp. 273–278, 1999.

[30] W. Barber, J. Wessel, N. Malakhov et al., "Energy dispersive photon counting detectors for breast imaging," in *Medical Applications of Radiation Detectors III*, vol. 8853 of *Proceedings of SPIE*, September 2013.